Investigations of poloidal velocity and shear in the SOL of ASDEX Upgrade

S. Costea[1], A.H. Nielsen[2], V. Naulin[2], J.J. Rasmussen[2], H.W. Müller[3], G.D. Conway[3], N. Vianello[4], D. Carralero[3], R. Schrittwieser[1], F. Mehlmann[1], C. Lux[1], C. Ionita[1], ASDEX Upgrade Team[3]

[1]*Institute for Ion Physics and Applied Physics, Fusion-ÖAW, University of Innsbruck, Austria*
[2]*Department of Physics, DTU, Kongens Lyngby, Denmark*
[3]*Max-Planck-Institute for Plasma Physics, Garching Germany*
[4]*Consorzio RFX, Padova, Italy*

1. Introduction

We have estimated the poloidal velocity and the position of the shear layer in the scrape-off layer of ASDEX Upgrade by five methods, using the six-pin reciprocating "Innsbruck-Padua" probe [1]. The poloidal velocity was estimated from *(i)* the $\boldsymbol{E}_r\times\boldsymbol{B}_t$ drift, where the local radial electric field was determined from the difference of the floating potentials of two radially separated cold pins, *(ii)* the cross-correlation (CC) and *(iii)* the conditional-average (CA) of two poloidally separated pins measuring the ion saturation currents, *(iv)* from the CC and *(v)* CA of two poloidally separated cold pins measuring the floating potentials. The results are compared with microwave Doppler reflectometry and ESEL simulation.

The investigated plasma discharge is #28877, having the following parameters:

Type	I_p (MA)	n_e (m^{-3})	B_t (T)	P_{ECRH} (MW)	q_{95}	Flat top time (s)
L-mode	1,00	$4{,}07\cdot10^{19}$	–2,43	0,484 (1,5-5,1 s)	4,105	1,12-5,25

During the flat top time of the plasma current, four insertions of the mid-plane manipulator were performed with the Innsbruck-Padua probe. In this paper, we present results from the inward motion of insertion *#1* and *#4*, at t = 2,1 s and at t = 4,8 s, respectively.

2. Experimental results

For the $\boldsymbol{E_r}\times\boldsymbol{B_t}$ method, the radial electric field was derived from two radially-separated cold pins (pins 6 and 8 in Fig. 1) which measured the floating potential. The mean $\boldsymbol{E}\times\boldsymbol{B}$ velocity has been derived from the potential difference divided by the radial distance between the pins (3 mm) and by the value of the magnetic field strength in the SOL (about –1,92 T with only 2% variation over the SOL).

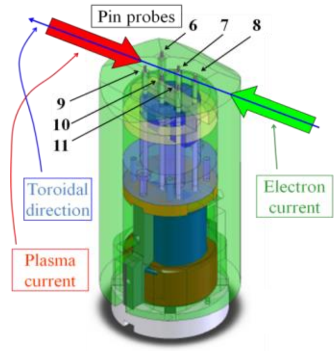

Fig. 1: The "Innsbruck-Padua" probe head (50 mm diameter, 115 mm length) having six probe pins of 1 mm diameter and 2 mm length each.

Both cross-correlation and conditional-average methods were performed with a moving window of 4000 data points (2 ms) on the fluctuating parts of the ion saturation currents (pins 7 and 10) and floating potentials (pins 8 and 11), with the poloidal separation of the pins being 10 mm. For the conditional-average method, we applied the condition on the amplitude of the signal on one pin to be larger than 2 times its standard deviation; then the sampling starts on the signal of its corresponding poloidally separated pin. The profiles are mapped to the normalized flux surface coordinate ($\rho_{poloidal}$) and the sign is with respect to the ion diamagnetic drift direction.

In Fig. 2 we present results for the poloidal velocity estimated by the aforementioned methods and the comparison with microwave Doppler reflectometry [2], during insertion *#1* and *#4* of the probe head into the plasma.

The estimated $\boldsymbol{E}\times\boldsymbol{B}$ drift velocity at $\rho_{poloidal}$ > 1,005 is nearly zero or negative despite that the other methods, including the Doppler diagnostics, estimate v_{pol} > 0,1 km/s. We believe

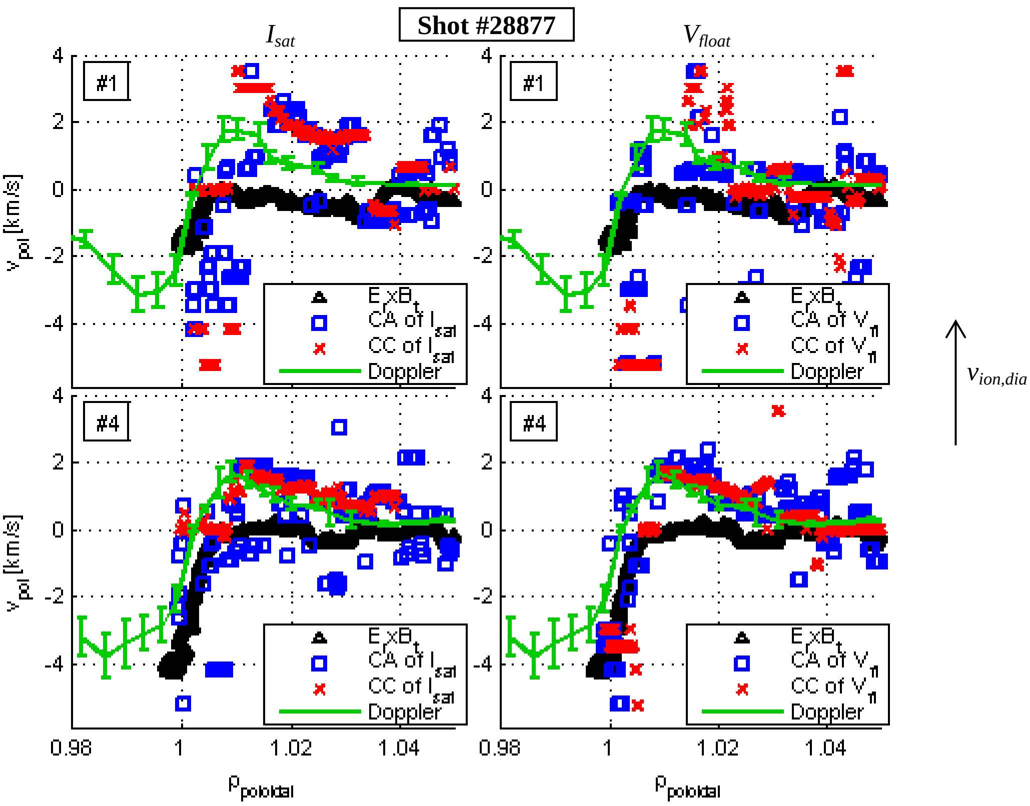

Fig. 2: Poloidal velocity vs. normalized flux surface coordinate during insertion #1 and #4. Probe data are represented by the symbols: red crosses for cross-correlation, blue squares for conditional-averaging and black triangles for $\boldsymbol{E}_r\times\boldsymbol{B}_t$*. Comparison with microwave Doppler reflectometry (green line). Left panels: CC and CA from ion saturation current, pins 7 and 10. Right panels: CC and CA from floating potential, pins 8 and 11.*

that here the temperature gradient is comparable to the plasma potential gradient. Close to separatrix, the potential gradient seems to be less affected by the temperature gradient therefore giving a better estimation of the radial electric field using 2 radially separated cold pins.

The position of the shear layer (i.e. strong gradient of poloidal velocity, Fig. 2, $\rho_{poloidal}$ = 1,005) determined by CC and CA on both ion saturation current and floating potentials are slightly outward in comparison with microwave Doppler reflectometry. This difference is within the uncertainty ($\Delta\rho_{poloidal} \approx 0{,}005$) to locate the separatrix by equilibrium reconstruction but also expected due to the fact the midplane manipulator is sitting at different toroidal coordinate than the microwave Doppler reflectometer.

3. Simulation results

The numerical code used to simulate the ASDEX Upgrade plasma is the ESEL code of the Technical University of Denmark. ESEL is a 2-dimensional interchange turbulence code which simulates the edge-SOL regions on the outboard midplane of a tokamak in the radial-poloidal plane (slab geometry). It makes use of an electrostatic fluid model which solves the equations for continuity, momentum and electron temperature [4].

A virtual probe head consisting of poloidally and radially separated synthetic point-pins was used to simulate the experimental probe head and the recorded signals. The synthetic signals provided by the simulation on each synthetic pin are: plasma potential, plasma density, electron temperature and poloidal flow velocity. From these, the synthetic normalized ion saturation current (I_{sat}) and the synthetic floating potential (V_{fl}) signals are constructed:

$V_{fl} = V_p - 3{,}2 \cdot T_e$, with V_p being the plasma potential and T_e the electron temperature.

$I_{sat} \sim n_p \sqrt{T_e}$ with n_p being the plasma density.

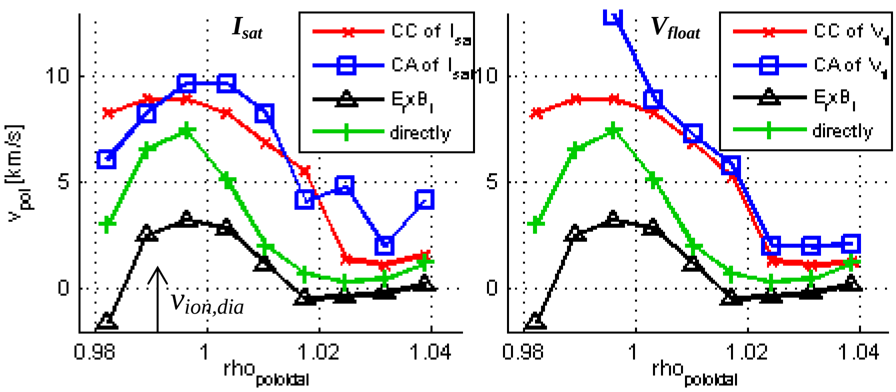

*Fig. 3: Synthetic poloidal velocity vs. normalized flux surface coordinate. Red crosses for cross-correlation, blue squares for conditional-averaging, black triangles for **E**×**B** and green crosses for the true simulated flow. Left panel: CC and CA from ion saturation current. Right panel: CC and CA from floating potential.*

CC, CA and **E**×**B** methods are applied to these synthetic probe signals and compared to the "real" flow as obtained by the simulation (Fig. 3).

CC and CA applied to synthetic signals show velocities slightly higher than the one delivered directly by the simulation. Furthermore, the position of the shear layer derived from these methods is slightly further outward compared to the "real" simulated shear layer, probably due to many-scale perturbations which may also have phase velocities [3].

4. Conclusions

CC does not always agree accurately with Doppler reflectometry (Fig. 1, #1), regardless whether ion saturation current or the potential are used, probably due to many-scale perturbations not all ‘frozen’ into the flow [3]. CA applied on experimental signals gives highly scattered results due to the combined effect of very poor statistics due to small number of events in the desired time window and the strong weight to the propagation of the high amplitude structures which do not always follow the flow [3].

There is visible change in the experimental results between insertions *#1* and *#4*, the latter one being closer to the Doppler reflectometry results. It is unclear whether this is due to a changed collisionality at increased plasma density.

Since the probe head manipulator is located above the midplane, the poloidally separated probes applied in the CC and the CA methods will not be on the same flux surface and this misalignment can influence the results as recent investigations have demonstrated [5].

The simulation could recreate the shape of the experimental profiles but they are slightly shifted towards the core plasma. This is due to the condition used in the model to locate the separatrix, i.e. there are no parallel loses at $\rho_{poloidal} < 1$ and there are losses at $\rho_{poloidal} > 1$. This condition does not create $\boldsymbol{E}_r = 0$ at $\rho_{pooidal} = 1$ but a little more towards core plasma.

There are some limitations to the model used in this work such as the details of the magnetic geometry, the role of sheaths and the presence of neutrals and impurities [4].

Acknowledgements

This project has received funding from the European Union's Horizon 2020 research and innovation programme under grant agreement number 633053. The views and opinions expressed herein do not necessarily reflect those of the European Commission. This work was also supported by grant P19901 of the Austrian Science Fund (FWF).

References

[1] C. Ionita *et al., J. Plasma Fusion Res. Series* **8**, 413 (2009).

[2] G.D. Conway *et al., Plasma Fusion Res.* ***5***, S2005, 6pp (2010).

[3] H.W. Müller *et al., Nucl. Fusion* **51** 073023 (2011).

[4] O.E. Garcia *et al., Plasma Phys. Contr. Fusion* **48**, L1 (2006).

[5] J. Madsen, *private communication*